ORIGINAL ARTICLE

Novel Trench Isolation Technology for Suspended MEMS Structures

Wen-Cheng Kuo[1,*] and Chih-Ming Liu[1]

[1] *Department of Mechanical and Automation Engineering, Nation Kaohsiung First University of Science and Technology, Taiwan, ROC*

(**Received** 9 December 2016; **Accepted** 07 February 2017; **Published on line** 1 March 2017)

*Corresponding author: rkuo@nkfust.edu.tw

DOI: 10.5875/ausmt.v7i1.1316

Abstract: This study presents a parylene-based trench isolation (PBTI) method using standard silicon wafer to obtain a suspended MEMS structure. The silicon-based suspended structures were electrically isolated using supported parylene beams. The parylene beams provide electrical isolation between the suspended structure and substrate, and prevent anchor movement during actuation and wire-bonding. The proposed process is a simple low-temperature, dry-etching and reliable fabrication method for structure creation and electrical isolation and does not require wet-release, LPCVD, plasma-enhanced chemical vapor deposition (PECVD), ion implantation, sputtering process, or sandwiched oxide/polysilicon/metal isolation. The parylene beams were created by performing multiple steps of parylene deposition and removal inside a silicon mold. The trench etching, polymer deposition for sidewall protection, floor polymer removal, structure release, and polymer stripping steps were completed by modifying the etching or passivation steps of the Bosch process. These steps can be integrated into a single-run ICP process controlled by macro commands; the ICP etcher can automatically complete suspended structure creation in a single run. A test device with a thickness of 50 μm and a maximum trench aspect ratio of 10 was created to demonstrate process feasibility. The proposed process can be used for sensors and actuators, requiring a considerable device thickness to enhance sensitivity and performance. The test device is a comb-drive like device used to check the electrical isolation for sensor and actuator. Design, simulation, and fabrication considerations are discussed.

Keywords: bulk micromachining, deep reactive ion etching (DRIE), high-aspect-ratio structure

Introduction

The well-established mechanical properties of single-crystal silicon (SCS) make it an excellent material for use in MEMS sensors and actuators, which require significant device thickness to enhance sensitivity and performance, thus raising the need for a suspended high-aspect-ratio structure (HARS) with satisfactory electrical isolation.

In suspended HARSs, structure depth is defined through deep reactive ion etching (DRIE) processes, such as the Bosch process [1], which comprise alternating etching and passivation steps. Several approaches have been used for structure release and electrical isolation, including single-crystal reactive etching and metallization (SCREAM) [2], the black silicon method (BSM) [3], the silicon-on-insulator (SOI) process [4], surface/bulk micromachining (SBM) [5], the dissolved wafer process (DWP) [6], the boron etch-stop assisted lateral silicon etching (BELST) process [7], the aluminum interconnect process for air-gap-insulated microstructures (AIM) [8], the polymer sidewall protection process for trench isolation technology [9], and the polymer sidewall protection process [[10]]. SOI and BSM processes involve the use of the buried oxide layer as the sacrificial layer for wet release. These are simple processes for structure release and are easy to control. However, the cost of these two wafers is excessively greater than standard silicon wafers. The suspended structures released by the DWP process have high dopant concentrations; therefore, they usually exhibit inferior mechanical properties. The processes proposed in ref. [2] and ref. [5]-[10] require extra fabrication steps for structure release or electrical isolation, such as plasma-enhanced chemical vapor deposition (PECVD), ion implantation, or sputtering. SOI is mostly used to reduce the complexity of industrial processes, but the high cost has motivated researchers to

develop a simpler alternative process using standard silicon wafer.

This study proposes a simple parylene-based trench isolation (PBTI) process using standard silicon wafer to fabricate suspended MEMS structures. The silicon-based MEMS structures are electrically isolated and suspended using parylene beams on the silicon substrate. The parylene beams provide electrical isolation between the suspended structure and substrate, and prevent anchor movement during actuation and wire-bonding. The proposed PBTI process enhances the polymer sidewall protection for trench isolation technology [9] because the trench isolation material from LPCVD low-stress silicon nitride is changed to parylene (polypara-xylylene). By changing the isolation trench material from silicon nitride to parylene, a change from a high-temperature (approximately 800 °C) LPCVD process to room-temperature (approximately 20 °C) parylene deposition can be achieved. Also, the beam width can increase from 2 to 20 μm to intensify the anchor stiffness. The proposed PBTI process is a simple low-temperature, dry-etching and reliable fabrication process for structure release and electrical isolation that does not require wet-release, LPCVD, PECVD, ion implantation, a sputtering process, or sandwiched oxide/polysilicon/metal isolation.

Parylene is used as a trench isolation material because of its chemical inertness, thermal stability, and compatibility with microfabrication technology [11]. Parylene can be deposited by pinhole-free conformal chemical vapor deposition coating at room temperature, and can be dry-etched using oxygen plasma [11].

Traditionally, parylene is deposited as a coating in thin-film materials. Suzuki et al. [13]-[15] proposed using a silicon micro-trench as a mold. By depositing and removing the parylene deposition inside the trenches, void-free parylene beams could be created as the trench isolation beam. The proposed PBTI-HARS method to create parylene (parylene-C) beams for structure release and electrical isolation.

Figure 1 shows a schematic diagram of parylene beam fabrication. First, parylene is deposited inside the silicon trench, as shown in Fig. 1(a). As shown in Fig. 1(b), the parylene deposition is conformal, and the film thickness is almost uniform even inside the deep trench. This is because the mean free path of parylene molecules is as small as a few cm, and also because the sticking coefficient, defined as the ratio between the number of molecules reacting with a radical chain end and the number of incident monomer molecules on the surface, is as low as $1x10^{-4}$ at room temperature [13]. In Fig. 1(c), the difference in the deposition rate between the top and bottom trenches causes the step coverage effect around the trench edges during deposition, thus the thickness in the corners of the trench is greater than that along the sidewall, increasing the likelihood of sealing the trench in a single run through the deposition of thick parylene layers. To prevent the trench from being sealed, oxygen plasma is applied to remove the uppermost parylene layer, thereby reopening the trench, as shown in Fig. 1(d). A second parylene layer is deposited to fill the trench without a void, as shown in Fig. 1(e). Oxygen plasma is applied again to clean the topmost section of parylene to form the parylene beam (Fig. 1(f)).

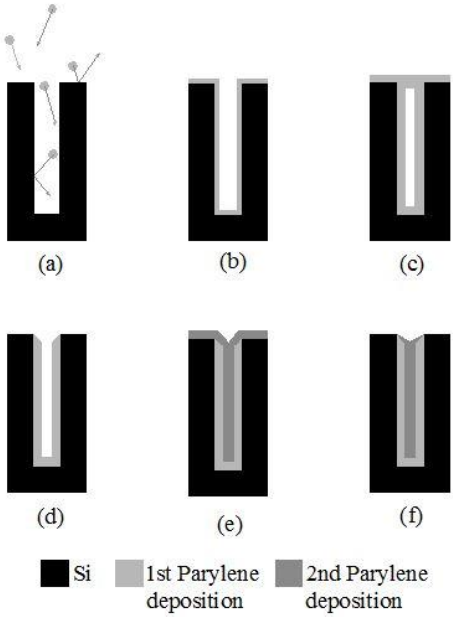

Figure 1. Schematic of the principle of the parylene beam creation. Step (a): parylene molecules start deposition inside the silicon trench; Step (b): parylene conformal deposition inside the silicon trench; Step (c): trench sealing by the difference in the deposition rate between the top and bottom trench; Step (d): opening the trench by oxygen plasma etching; Step (e): a second parylene deposition to fill the trench without a void; Step (f): oxygen plasma is applied again to clean the topmost section of parylene to form the parylene beam.

After the parylene-based electrical isolation beams are created, the modified Bosch process [9], [10] is applied to fabricate the suspended MEMS structure through an inductively coupled plasma-reactive ion etching (ICP-RIE) process. The trench etching, sidewall protection, floor polymer removal, structure release, and polymer stripping steps can be completed by modifying the etching or passivation steps of the Bosch process. These steps can be integrated into a single-run ICP process controlled by macro commands; the ICP etcher can automatically finish the suspended structures creation in a single run. The silicon-based structures are electrically isolated by supported parylene beams. The proposed process can be used for sensors and actuators, which require a considerable device thickness to enhance sensitivity and performance. A test device was fabricated and is discussed.

The remainder of this paper is organized as follows: Section 2 presents the process design, including the parylene isolation beams, silicon-suspended structures,

and their relative dimensions. Section 3 presents fabrication considerations. Section 4 discusses the fabrication results of the test device. Section 5 offer conclusions.

Process design

Figure 2 shows the proposed fabrication process. Eight steps containing two masks were required for the process. A 4-in SCS wafer was used without considering crystallographic orientation. The following section provides detailed descriptions of these steps.

- Step (1): First PR patterning and trench etching

  In this step, a photoresist (PR) is spun on the wafer, followed by a pattern process. The standard Bosch process is then applied to etch the exposed silicon to the desired depth.
- Step (2): PR removal and parylene beam creation

  Oxygen plasma is applied to remove the PR. The trenches generated in Step (1) are used as the mold; by depositing and removing the parylene (parylene-C) inside the trenches, void-free parylene beams can be created inside them.
- Step (3): Top layer parylene removal and second PR patterning

  Oxygen plasma is applied to remove the top parylene layer, exposing the silicon surface, and the PR of the suspended silicon structures is patterned.
- Step (4): Second trench etching

  In this step, the exposed silicon is etched using the standard Bosch process to define the structure thickness before structure release.
- Step (5): Polymer deposition

  After the trenches are created, the modified Bosch process is applied. By using only the passivation step, the fluorocarbon polymer layer is deposited around the structure surface so that the sidewalls of the trenches are protected during the following structure release step.
- Step (6): Floor polymer removal

  In this step, the Bosch process is modified using only the etching step. The etchants (fluorine and oxygen radicals) generated in this step are used to remove the floor polymer with the assistance of ion bombardment.
- Step (7): Structure release

  In this step, the Bosch process is modified using the etching step only, and the platen power is closed. The exposed silicon is isotropically etched, and the structures are released at the trench bottom.
- Step (8): Polymer stripping

  In this step, the photoresist and most of the passivation layers can be removed using oxygen plasma.

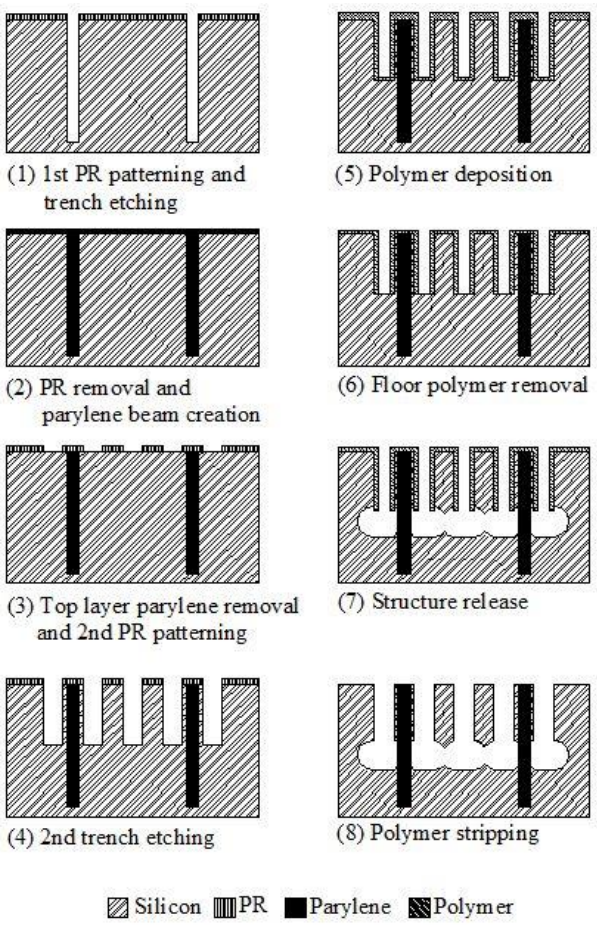

Figure 2. Proposed process schematic.

Figure 3 shows the relationship between the dimensions of the parylene-based electrical isolation beams and those of the silicon-based suspended structure. To achieve reliable electrical isolation, the isolation trench depth (d_1) for the first trench etching step, the structure trench depth (d_2) for the second trench etching step, the release width of isolation beam (w_1), the maximum suspended structure width (w_2), the minimum etching distance (r), the structure thickness (h), and the supported anchor depth (d_3) must all be selected in accordance with each other. Table 1 shows the dimensions chosen for the test device.

Assuming that the release process is completely isotropic, the minimum etching distance (r) must be longer than a half width of the structure (w2) and the release width of isolation beam (w1) to completely undercut it; that is,

$$r = vt \geq w_1 = \frac{w_2}{2} \tag{1}$$

where v is the isotropic etching rate, and t is the time required to release the structure.

The required trench depth (d_2) for the second trench etching step is equal to

$$d_2 = h + r \geq h + w_1 = h + \frac{w_2}{2} \quad (2)$$

The required isolation trench depth (d_1) for the first trench etching step is equal to

$$d_1 = h + 2r + d_3 \geq h + 2w_1 + d_3 = h + w_2 + d_3 \quad (3)$$

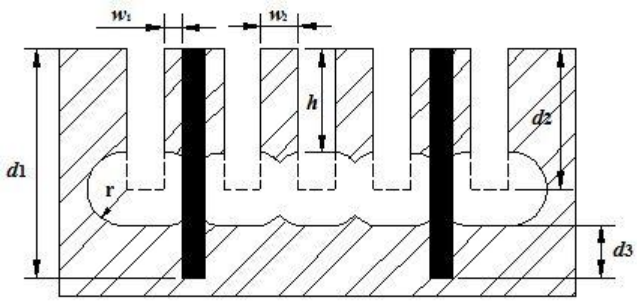

Figure 3. Parameter design for the suspended high-aspect-ratio structure.

Table 1. Test device dimensions.

Item	Dimension (μm)
Isolation trench depth (d_1) for 1st trench etching	120
Structure trench depth (d_2) for 2nd trench etching	70
Release width of isolation beam (w_1)	20
Maximum suspended structure width (w_2)	40
Minimum etching distance (r)	20
Structure thickness (h)	50
supported anchor depth (d_3)	30

To meet the requirements of parylene beam creation, the designed isolation beam width was 20 µm. For a maximum suspended structure width (w2) of 40 µm, the supported anchor depth (d3) was 30 µm. To attain a 50 µm structure thickness (h), the calculated minimum isolation trench depth (d1) for the first trench etching step and the structure trench depth (d2) for the second trench etching step were respectively 120 µm and 70 µm.

Concerning the spacing arrangement of the parylene electric insulation beams, the crossed spacing for the anchors was designed as shown in Fig. 4, where the release width of the isolation beam (w_1) is 20 µm, the parylene width is 20 µm, and the release trench and hole are respectively 30 and 30X30 µm. Figure 5 shows the spacing arrangement of the parylene electric insulation beams for the test device (comb-drive like actuator), where the widths of the parylene and silicon at the anchor/fixed comb are respectively 20 and 40 □m. The silicon width at the shuttle and flexible beam/comb finger are respectively 20 and 10 µm.

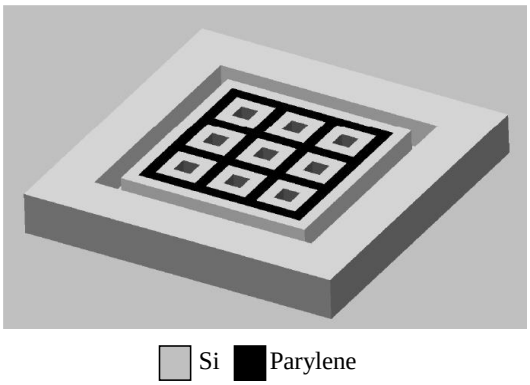

Figure 4. Spacing arrangement of parylene electric insulation beams.

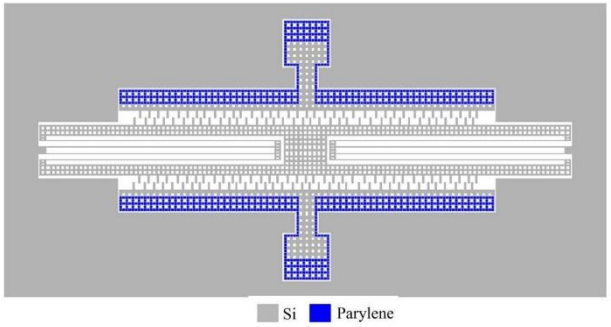

Figure 5. Actual spacing arrangement of parylene electric insulation beams for the test device.

To ensure that the stiffness of the parylene isolation beams was sufficient to prevent anchor movement and to support the suspended silicon structure under pressure load by actuating or wire-bonding, the simulation tool Coventorware® was used to verify the dimensions of the isolation beams and spacing. The Young's Modulus values for the silicon and parylene-C in the simulation are respectively 169 GPa and 4.7 GPa [16]. Figure 6(a) shows the large pressure load (0.1 MPa) to simulate the actuating force applied on the test device, and the layout and dimensions are respectively shown in Fig. 5 and Table 1. The pressure loading was applied on the sidewall of the suspended structure. The simulation checked the horizontal movement of the suspended structure during actuation. When a pressure of 0.1 MPa was applied to a patch with dimensions of 5000 × 50 µm, the maximum movement of the anchor was approximately 0.0038 µm. Figure 6(b) shows the pressure load of 0.04 MPa to simulate 15 g of wire-bonding force applied on top of the anchor with dimensions of 600 × 600 µm supported by the parylene beams. The simulation checked the vertical movement of the suspended structure by 15g of wire-bonding force. The maximum movement of the anchor was approximately 0.0037 µm. Based on the simulation results, this spacing design was acceptable.

Fabrication considerations

Following the proposed process shown in Fig. 2, Table 2 illustrates the fabrication of the test device using the single-run modified Bosch process. However, the polymer deposition, floor polymer removal, and structure release steps must be tested when using different suspended structure thicknesses.

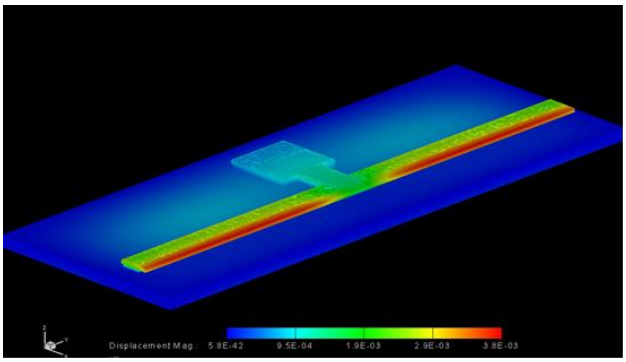

(a)

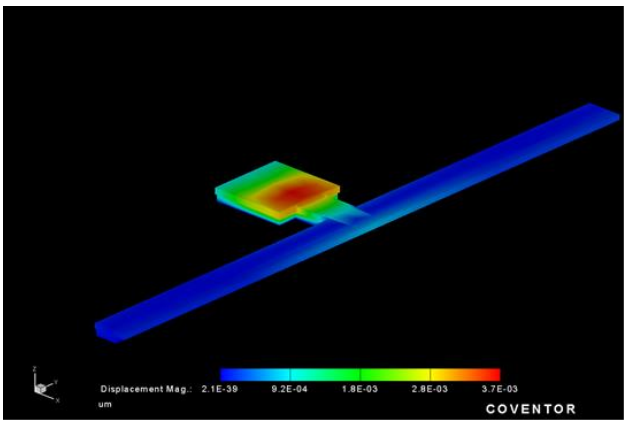

(b)

Figure 6(a): Deflection simulation for 0.1 MPa pressure loading applied to a patch with dimensions of 5000 × 50 µm. The simulation checks the horizontal movement of the suspended structure during actuation; Figure 6(b): Deflection simulation for 0.04 MPa pressure loading applied on the anchor with dimensions of 600 × 600 µm. The simulation checks the vertical movement of the suspended structure by 15g of wire-bonding force.

Because of the conductance effect [17, 18] and the reactant transport effect [19], in the polymer deposition step the width of the trench opening and the trench aspect ratio impacted the fluorocarbon (FC) deposition flux distribution. A larger trench opening or smaller trench aspect ratio resulted in a greater polymer deposition rate at the trench bottom [10]. Using the settings shown in Table 2, the thickness of the test device was 50 m, the trench aspect ratio was 10, and the respective polymer thicknesses on the top and bottom of the trench were approximately 2.6 m and 0.19 m.

In the floor polymer removal step, the etchant generated in the etching step of the Bosch process—consisting of fluorine and oxygen radicals—was used to remove the floor polymer with the assistance of ion bombardment. The removal time was carefully controlled to remove the floor polymer without affecting the top layer of the polymer. Excessive etching time would result in the corner of the top layer or the entire top layer of the polymer being etched, and the top layer of the structure would be destroyed in the following release step.

In the structure release step, according to (1), the release time (t) must be greater than w2/2v. However, because of the conductance effect and the reactant transport effect, the isotropic etching rate was lower for smaller trench openings or larger trench aspect ratios. Given an identical mask layout, the release time increases with device thickness. In this case, the thickness of the test device was 50 m and the trench aspect ratio was 10. Using the settings shown in Table 2, the release time was approximately 21 min.

Fabrication results

The proposed PBTI process was used to fabricate a test device with a thickness of 50 m. The deposition rate of parylene was about 0.04 m/min on the top of the structure. Figure 7(a) shows SEM images of the diced cross section of the parylene beam in step (4) of Fig. 2; these images verify that no voids remained inside the parylene beams. Figure 7(b) shows an SEM image of the cross-section of the silicon suspended structure to verify full structure release, and Figure 7(c) shows an SEM image of the cross-section of the silicon suspended structure with parylene isolation beams to indicate the difficulty of identifying horizontal shift in the top structure following structure release. Because of the small Young's Modulus of parylene, the suspended part of the parylene beams without silicon support easily filled the etched cavities downstream of the parylene beams. Figures 8(a) and (c) show the SEM images of the test structure before PR stripping, and Figs. 8(b) and (d) show the SEM images of the test structure after PR stripping. Figure 9 shows an SEM image of the fabricated test device, a comb-drive like device for checking the electrical isolation of sensors and actuators.

Conclusion

This paper presents the design, simulation, and fabrication of PBTI process for MEMS suspended structures. The silicon-based structures were electrically isolated using supported parylene beams. The parylene-based electrical isolation beams were created through

Table 2.Single-run Bosch process recipe.

Process step	Coil power (Watt)	Platen power (Watt)	Gases flow (sccm) $SF_6/O_2/C_4F_8$	Pressure (mT)	Time (Minute)
1. Trench etching	*	*	*	*	*
2. Polymer deposition	600	0	0/0/99	23	28
3. Floor polymer removal	600	15	130/13/0	15	4
4. Structure release	600	0	195/13/0	45	21
5. Polymer striping	600	15	0/99/0	7	12

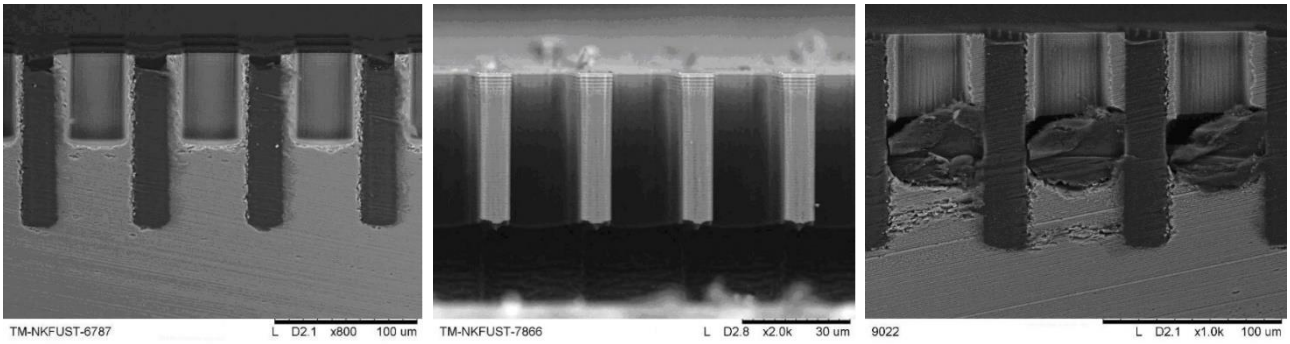

(a) (b) (c)

Figure 7 (a): Cross-sectional SEM image of the parylene beam by dicing in step (4) of Fig. 2 with void-free parylene beams. Figure 7(b): Cross-sectional SEM image of the silicon suspended structure with fully structure release. Figure 7(c): Cross-sectional SEM image of the silicon suspended structure with parylene isolation beams without horizontal shift after structure release.

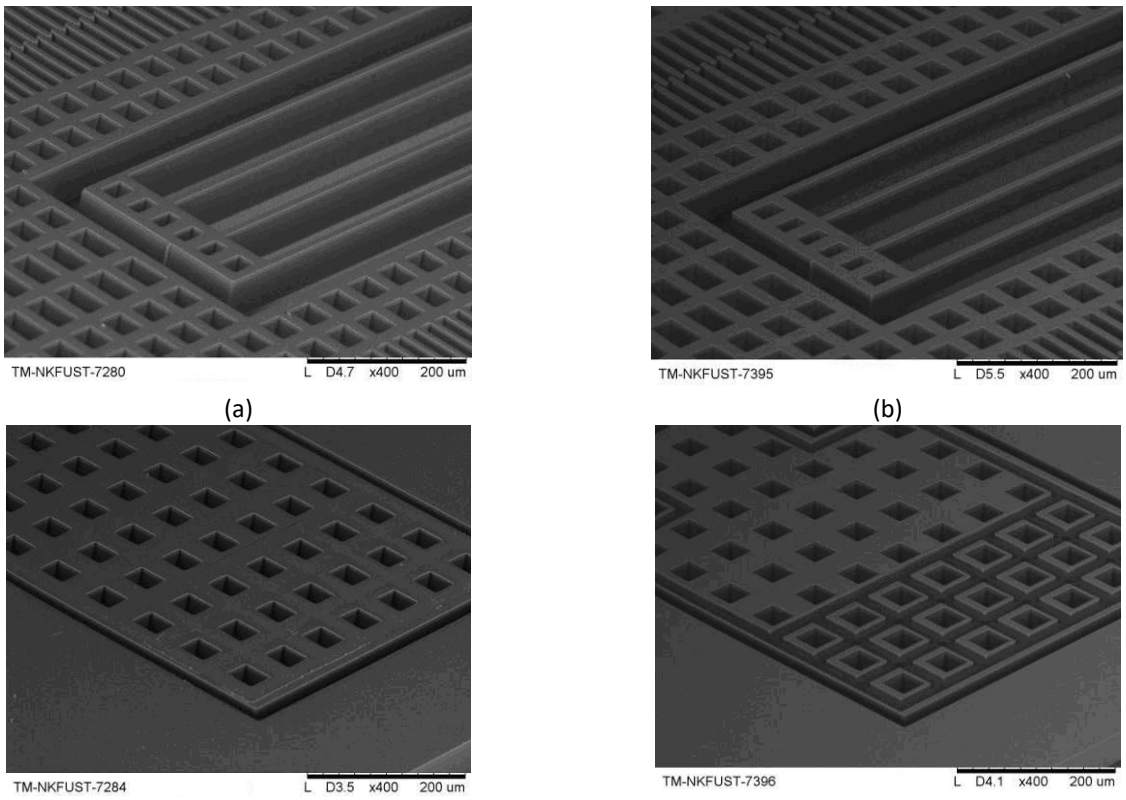

(a) (b)

(c) (d)

Figure 8. SEM images of the test structure: (a) and (c) before top side polymer removal; (b) and (d) after top side polymer removal.

multiple steps of parylene deposition and removal inside the silicon mold. The trench etching, sidewall protection, floor polymer removal, structure release, and polymer stripping steps were completed by modifying the etching or passivation steps of the Bosch process. These steps can be integrated into a single-run ICP process controlled by macro commands; the ICP etcher can automatically finish the suspended structures creation in a single run. A test device with a thickness of 50 m and a maximum trench aspect ratio of 10 was fabricated to prove the feasibility of the process. The proposed process can be used for sensors and actuators, which require considerable device thickness to enhance sensitivity and performance. Design, simulation, and fabrication considerations are also discussed.

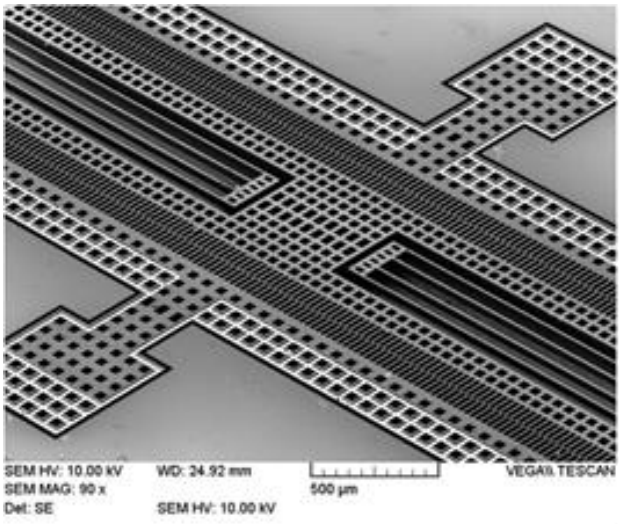

Figure 9. SEM images of the test structure.

Acknowledgment

The authors appreciate the financial support of the National Science Council of Taiwan (NSC 98-2221-E-327-035 and NSC 99-2221-E-327-035).

References

[1] F. Laermer and A. Schilp, "A Method of anisotropically etching silicon," *US Patent* 5501893 , 1996.

[2] K. A. Shaw, Z. L. Zhang, and N. C. MacDonald, "SCREAM I: A Single mask, single-crystal silicon, reactive ion etching process for microelectromechanical structures," *Sensors and Actuators A*, vol. 40, no. 1, pp. 63-70, 1994. doi: 10.1016/0924-4247(94)85031-3

[3] M. de Boer, H. Jansen, and M. Elwenspoek, "The black silicon method V: A study of the fabricating of movable structures for micro electromechanical systems," in proceeding of *the 8th International Conference on Solid-State Sensors and Actuators (Transducers '95)*, Amsterdam, Netherlands, June 25-29, 1995, pp. 565-568. doi: 10.1109/SENSOR.1995.717287

[4] B. Diem, M. T. Delaye, Michel, F. Renard, and G. Delapierre, "SOI(SIMOX) as a substrate for surface micromachining of single crystalline silicon sensors and actuators," in proceeding of *the 7th International Conference on Solid-State Sensors and Actuators (Transducers '93)*, Yokohama, Japan, June 7-10, 1993, pp. 233-236.

[5] S. Lee, S. Park and D. Cho, "The Surface/Bulk Micromachining (SBM) process: A new method for fabrication released MEMS in single crystal silicon," *Journal of Microelectromechanical System*, vol. 8, no. 4, pp. 409-416, 1994. doi: 10.1109/84.809055

[6] Y. B. Gianchandani and K. Najafi, "A bulk silicon dissolved wafer process for microelectromechanical devices," *Journal of Microelectromechanical System*, vo. 1, no. 2, pp. 77-85, 1992. doi: 10.1109/84.157361

[7] J. Hsieh and W. Fang, "A boron etch-stop assisted lateral silicon etching process for improved high-aspect-ratio silicon micromachining and its applications," *Journal of Micromechanical Microengineering*, vol. 12, no. 4, pp. 574-581, 2002. doi: 10.1088/0960-1317/12/5/310

[8] A. Bertz, M. Kuechler, R. Knoefler, and T. Gessner, "A novel high aspect ratio technology for MEMS fabrication using standard silicon wafers," *Sensors and Actuators A*, vol. 97-98, no. 1, pp. 691-701, 2002. doi: 10.1016/S0924-4247(02)00006-7

[9] E. Sarajlic, M. J. de Boer, H. V.Jansen, N. Arnal, M. Puech, G. Krijnen, and M. Elwenspoek, "Advanced plasma processing combined with trench isolation technology for fabrication and fast prototyping of high aspect ratio MEMS in standard silicon wafers," *Journal of Micromechanical Microengineering*, vol. 14, no. 9, pp. 70-75, 2004. doi: 10.1088/0960-1317/14/9/012

[10] Y.-J. Yang, W.-C. Kuo, and K.-C. Fan, "Single-run single-mask inductively- coupled-plasma reactive-ion-etching process for fabricating suspended high-aspect-ratio microstructures," *Japanese Journal of Applied Physics*, vol. 45, part 1, no. 1A, pp. 305-310, 2006. doi: 10.1143/JJAP.45.305

[11] A. Tooker, E. Meng, J. Erickson, Y. C. Tai and J. Pine, "Development of biocompatible parylene neurocage," in proceeding of *the 26th Annual International Conference IEEE Engineering in*

Medicine and Biology Society (EMBC), San Francisco, USA, Sept. 1-5, 2004, pp. 2542-2545.
doi: 10.1109/IEMBS.2004.1403731

[12] V. S. Kale and T. J. Riley, "A production Parylene coating process for hybrid microcircuits," *IEEE Transaction on Parts, Hybrids, and Packaging*, vol. 13, no. 3, pp. 273-279, 1997.
doi: 10.1109/TPHP.1977.1135214

[13] Y. Suzuki and Y. C. Tai, "Micromachined high-aspect-ratio parylene spring and its application to low-frequency accelerometers," *Journal of Microelectromechanical System*, vol. 15, no. 5, pp. 1364-1370, 2006.
doi: 10.1109/JMEMS.2006.879706

[14] Y. Feng, K. Hagiwara, Y. Lgchi, and Y. Suzuki, "Trench-filled cellular parylene electret for piezoelectric transducer," *Applied Physics Letters*, vol. 100, no. 26, pp. 262901-262904, 2012.
doi: 10.1063/1.4730952

[15] R. Chen and Y. Suzuki, "Suspended electrodes for reducing parasitic capacitance in electret energy harvesters," *Journal of Micromechanical Microengineering*, vol. 23, no. 12, pp. 125015-125022, 2013.
doi: 10.1088/0960-1317/23/12/125015

[16] W.-C. Kuo, C.-W. Chen, and C.-M. Liu, "Design and fabrication of a high-aspect-ratio parylene-based comb-drive actuator for large displacements at a low driving force," *Journal of Micromechanical Microengineering*, vol. 23, no. 6, pp. 065021-065027, 2013.
doi: 10.1088/0960-1317/23/6/065021

[17] S. Dushman and J. M. Lafferty, Scientific Foundations of Vacuum Technique, 2nd ed., New York, Wiley: 1962, pp. 94.

[18] J. W. Coburn and H. F.Winters, "Conductance considerations in the reactive ion etching of high aspect ratio features," *Applied Physics Letters*, vol. 55, no. 26, pp. 2730-2732, 1989.
doi: 10.1063/1.101937

[19] J. C. Arnold, D. C. Gary, and H. H. Sawin, "Influence of reactant transport on fluorine reactive ion etching of deep trenches in silicon," *J. Vac. Sci. Technol. B Nanotechnol. Microelectron.*, vol. 11, no. 6, pp. 2071-2780, 1993.
doi: 10.1116/1.586545